Estonian Journal of Engineering, 2013, **19**, 2, 124–142 doi: 10.3176/eng.2013.2.03

Exposure of a coastal city to a landslide tsunami: a case study of Cassis, France

Elena Averbukh[a], Philippe Dussouillez[b], Christian Kharif[c], Olga Khvostova[d], Andrey Kurkin[a], Pierre Rochette[b] and Tarmo Soomere[e,f]

[a] Nizhny Novgorod State Technical University n.a. R. E. Alekseev, Minin St. 24, 603950 Nizhny Novgorod, Russia; averbukh.lena@gmail.com
[b] CEREGE, Aix Marseille University CNRS, Europole de l'Arbois, 13545 Aix-en-Provence cedex 4, France; rochette@cerege.fr
[c] Ecole Centrale Marseille, 13545 Marseille Cedex 20, France; kharif@irphe.univ-mrs.fr
[d] National Research University Higher School of Economics, 136 Rodionov St., 603093 Nizhny Novgorod, Russia; okhvostova@hse.ru
[e] Institute of Cybernetics at Tallinn University of Technology, Akadeemia tee 21, 12618 Tallinn, Estonia; soomere@cs.ioc.ee
[f] Estonian Academy of Sciences, Kohtu 6, 10130 Tallinn, Estonia

Received 29 April 2013, in revised form 28 May 2013

Abstract. The rise of sea level will enhance erosion of cliffs that will be in the reach of storm waves in the distant future. We analyse the possible consequences of erosion-driven collapse of the cliff of Cap Canaille, located approximately 20 km from Marseille, France. A resulting fall of large amount of rocks (several millions m^3) into the sea (or a subaerial landslide of an equal volume) may generate a local tsunami that will endanger the adjacent seaside resort Cassis. The propagation of waves, created by this hypothetic event, is simulated using the fully non-linear Boussinesq wave model FUNWAVE. The maximum elevation in Cassis may reach 3.6 m and it only weakly depends on the particular scenario of the collapse. The largest source of danger is the short arrival time (3–3.5 min) of the first wave that is also the highest one. This requires implementation of non-traditional means for building resilience of the local coastal community with respect to such events.

Key words: landslide tsunami, tsunami modelling, Boussinesq equations, Cassis, Cap Canaille, tsunami resilience.

1. INTRODUCTION

It is well known that one of the key consequences of the global warming is the rise of sea level [1]. Additionally to problems associated with flooding of low-level areas [2], degradation of barrier islands [3] or enhanced coastal erosion [4], this process impacts also seemingly stable cliffed coasts [5]. These coasts retreat

at a certain rate [6] that in many occasions is only moderately smaller than the rate of retreat of, for example, till coasts [7,8]. The largest threat to such coasts is that owing to the sea level rise the cliff toe may become subject to direct wave impact. The results of such an impact may remain unnoticed for a while for the retreat of such cliffs is a step-like process [5,6]. Such a delay of the visible consequences together with an increase of the effective water depth at the toe of the cliff leads to an increased risk of collapse of large sections of the cliff into water of considerable depth. The largest danger associated with such an event is its potential to generate a devastating tsunami.

Tsunamis induced by subaerial landslides are thought to be the highest among contemporary tsunamis [9]. They have happened in several regions of the World Ocean also in the recent past. For example, on September 13, 1999, Omoa Bay (the Island of Fatu Hiva, French Polynesia) was struck by 2 to 5 m high waves [10]. The reason was the collapse into the sea of a relatively modest in size (300×300 m^2) at least 20-m thick cliff located 5 km southeast of Omoa. In particular, the striking amplification observed in Omoa Bay is related to the trapping of waves due to the shallow submarine shelf, surrounding the island. They do happen also in the European waters. On December 30, 2002 several destructive waves attacked the coast of the volcanic island of Stromboli, in the Tyrrhenian Sea [11]. These waves were excited by landslides of estimated volume of 10.8×10^6 m^3 [12] that took place on the north-west flank of the volcano along the steep slope of Sciara del Fuoco. The waves also damaged several sections of the Island of Linari, located about 40 km from the event.

There are many high cliffs and potentially unstable mountain slopes along the European coasts. While the related dangers are probably at best quantified for volcanic islands [13], this threat is intrinsically present also in several other domains [14]. The largest hazard in terms of exposure of people to such tsunami exists in cities that are located in the immediate vicinity of such cliffs and where such a "surprise tsunami" may arrive within a few tens of minutes without any apparent warning [15]. The above has shown that the radius of impact of such tsunamis may be several tens of kilometres.

A general discussion of risks, associated with tsunamis for the French coast of the Mediterranean, can be found in [16]. One site, potentially endangered by landslide-induced tsunami, is Cassis, a popular tourist town located near Marseille, France, well known for its wine too. There are several beautiful places for swimming and diving in the vicinity of Cassis. The surrounding landscape with high and bright cliffs has made it a favourite location of painters. The danger here is owing to the presence of one of the highest coastal cliffs (394 m) in Europe. It is located at Cap Canaille, close to Cassis (Fig. 1).

The foot of the cliff mostly consists of marly limestone. Presently the cliff does not show strong evidence of potential instability. There is, however, evidence that such collapses have occurred in this region in the past [17]. The remains of the collapsed blocks are clearly visible on the slope of the shoreline

(Fig. 2). The average cliff retreat velocity was estimated to be on the order of 5 m per millennium.

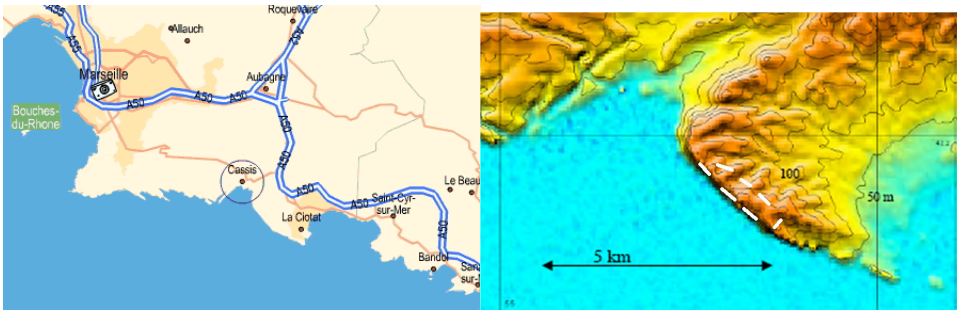

Fig. 1. Location scheme of the Cassis area (left panel); topography of cliffs of Cap Canaille (right panel, isolines at every 50 m; white dashed lines indicate the location of a potential landslide).

(a)

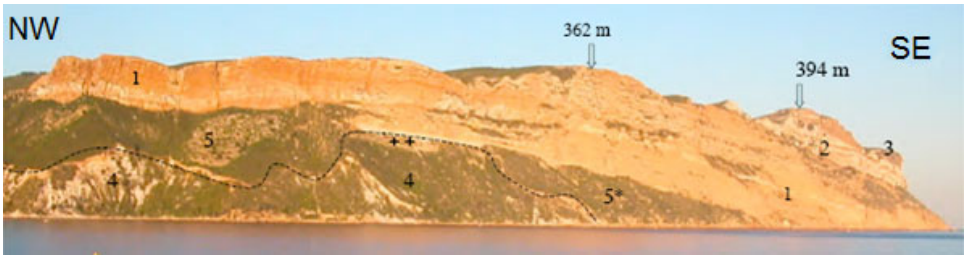

(b) (c)

Fig. 2. (a) A view of the cliff at Cap Canaille [17]. NW denotes the north-western and SE the south-eastern end of the cliff. The components of rocks are: 1 – calcareous sandstone; 2 – massive limestone; 3 – conglomerate; 4 – marl (under active erosion); 5 – stable ancient formation of fallen rocks. Dotted line indicates the boundary of the present marl mass under erosion. This formation reaches the cliff rock at a point marked by ++. The width of the entire formation is about 4 km; (b), (c) overhanging rocks on the steep slope. Photos by P. Rochette.

As the marl masses are located at the foot of the cliff, it is very likely that the predicted sea level rise in the near future may considerably accelerate the presently slow erosion of the marl slope and enhance the occurrence of the next collapse. The erosion of low-lying marl masses will eventually cause overhanging of the cliff and thus an increased level of danger by large waves, should a collapse occur.

In many locations a collapse of coastal cliffs or the formation of landslides along steep slopes in the immediate vicinity of the coastline has occurred owing to earthquakes (for example, on July 17, 1998, in the Papua New Guinea [18]). In these occasions the signal of such a large-scale disturbance is a natural sign of warning for a possible wave attack. The level of seismicity is, however, very low in the region of Cap Canaille. This means that a collapse of cliffs in this region owing to erosion of their foot is basically a random event that may be triggered by certain local circumstances. For this reason it is almost impossible to develop an early warning system and the resilience of the potentially affected domains should be built using certain preventive methods that account for the damaging potential of the tsunami caused by such a collapse.

The main goal of this paper is twofold. Firstly, we present results of numerical simulations of the tsunami wave, potentially caused by this future hypothetic event according to three viable scenarios. The presentation of this material follows the preliminary reports [19,20]. To adequately solve this problem, it is necessary to reasonably estimate the features of the hypothetic slump and following landslide. Secondly, we address the possibilities for proper reaction to such events and building resilience of coastal communities in situations where the wave may hit a touristic town within a few minutes after a collapse of the cliff.

2. STUDY AREA

The study area is located in the southern coast of France, about 20 km to south-east of Marseille in the vicinity of Cassis (Fig. 1). The focus is on the cliff of Cap Canaille (Fig. 2) located between Cassis and La Ciotat. The high cliff, facing the Mediterranean Sea, is about 4 km long. The cliff rocks contain several components such as calcareous sandstone in the north-eastern part of the area, massive limestone in the south-eastern part of the cliff and conglomerate at the southern end of the cliff (Fig. 2). A large part of the cliff foot is covered by masses of marl that extend down to the contemporary waterline and is subject of intense wave-driven erosion. At places, stable formations of rocks, fallen in the past, are found.

It is natural to assume that the following chain of events will pave the way to the collapse of the cliff. When the sea level increases, the enhanced wave impact will erode slowly the mass of marl (area 4 in Fig. 2) located at the foot of the cliff. This process is eventually enhanced by an increase in hydrostatic pressure and is additionally amplified because of an increase in the wave height at the cliff due to the increase in the water depth. After some time the cliff will hang over

the sea but will probably remain stable for some time. If the erosion continues, the breaking threshold is eventually reached, resulting in a massive collapse into the sea (Fig. 3). The estimated volume of the slide (that occurred about 3500 years ago), based on the dimensions of the cliff and properties of its rocks, is from 3×10^6 to 11×10^6 m^3 [17]. Although this amount of material evidently cannot drive a megatsunami [9], the volume of falling rocks is comparable to the volume of landslides at Stromboli. These landslides generated quite a powerful tsunami that led to extensive damage at a distance of a few kilometres and to a certain damage at a distance of some 40 kilometres [11].

We emphasize that a substantial tsunami wave may only occur if the collapse is a single catastrophic event (or a sequence of almost overlapping events occurring within one generated wave period), not a protracted sequence of smaller collapses. Studies of previous collapses of Cap Canaille have not strictly demonstrated which scenario of a potential landslide is most likely although indirect arguments were presented in favour of a single event [17].

A single-event collapse will eventually cause a local tsunami that will first hit the city of Cassis (Fig. 4), located just a few kilometres from the potential rockfall location. This city does have extensive coastal protection. Almost all its coastline is to some extent protected by seawalls. The old harbour (Fig. 4b) is protected by up to 4–5 m high breakwaters. Still, two beaches are fully open to the sea and to the potential tsunami. The larger of these two, with a steeply sloping nearshore, is located near the harbour (Fig. 4c) and another is located on the other side of the bay. In the case of an attack by a tsunami wave of even a moderate height (larger than 1–1.5 m), the harbour and the square adjacent to it will be inundated. It is very likely that numerous cafes and restaurants located in this area will be damaged, which means extensive danger to lives in this very popular area.

The extension of danger is somewhat limited due to the presence of three-floor buildings and narrow and steep streets that radiate from the square in question (Fig. 4d). These buildings and uphill streets together protect the rest of the city from the tsunami to some extent. Such a structure of the city means that the propagation of the tsunami wave will be relatively limited. Moreover, the wave is not likely to reach the second and third floors that may provide a shelter in case of actual wave attack.

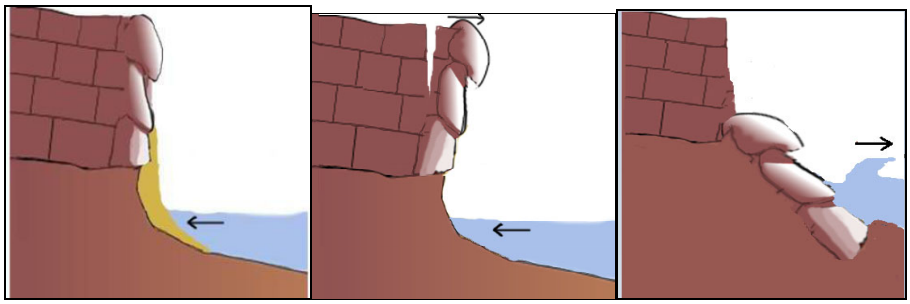

Fig. 3. Steps of erosion and rupture of the cliff, triggered by the sea level rise.

Fig. 4. View of Cap Canaille (a), view from the harbour of Cassis (b), the beach (c), radial narrow streets in Cassis (d), view of the city from Cap Canaille (e). Photos by O. Khvostova.

The level of danger for the other beach is smaller because its slope is steeper and there is only a small square adjacent to it. The square is additionally protected by a car bridge. The rest of the coastline of the city is protected by a 5–8 m high seawall that substantially reduces the danger associated with the tsunami attack. The presence of several virtually open coastal stretches that are highly

popular for both local people and visitors still means that this hypothetic event of cliff collapse and tsunami excitation may cause a significant number of fatalities in the city, especially around the harbour and on the beaches, which are hugely populated during the touristic season.

3. WAVE MODEL

We chose the public-domain FUNWAVE (version 1.0) package [21,22] to model the tsunami wave generation and propagation. This model is based on Boussinesq-type shallow water equations for wave propagation in two horizontal dimensions but it simulates realistic wave dispersion [23], bottom friction, basic fluid mechanics of breaking waves, and also wave run-up and inundation [24,25]. For practical applications, the model is equipped with options to replicate wave generation, boundary absorption and moving shoreline. This formulation provides a sound and well-tested against laboratory measurements [26] basis for the simulation of wave propagation in coastal region [27].

The equations of conservation of mass and momentum, employed in the version of the model used in this study, describe the frictionless evolution of non-breaking waves over a smooth, impermeable bottom and are as follows [27]:

$$\eta_t = E(\eta,u,v) + \gamma E_2(\eta,u,v) + f(x,y,t), \tag{1}$$

$$[U(u)]_t = F(\eta,u,v) + [F_1(v)]_t + \gamma[F_2(\eta,u,v) + F^t(\eta,u_t,v_t)] + F_b + F_{br} + F_{bs} + F_{sp}, \tag{2}$$

$$[V(v)]_t = G(\eta,u,v) + [G_1(u)]_t + \gamma[G_2(\eta,u,v) + G^t(\eta,u_t,v_t)] + G_b + G_{br} + G_{bs} + G_{sp}. \tag{3}$$

Here η is surface elevation, h is the still water depth, u and v are the horizontal velocities in the x- and y-direction, respectively. The quantity γ has the meaning of a control parameter allowing to choose between fully ($\gamma = 1$) or weakly ($\gamma = 0$) non-linear cases, g is the gravity acceleration and subscript t denotes the partial derivative with respect to time. In our simulations we have used the fully non-linear version with $\gamma = 1$. Detailed expressions for the functions U, V, E, E_2, F, F_1, F_2, G, G_1, G_2, F^t and G^t and source and sink terms $F_b, F_{br}, F_{bs}, F_{sp}$ and $G_b, G_{br}, G_{bs}, G_{sp}$ can be found in [27]. Equations (1)–(3) are integrated using a composite 4th-order Adams-Bashforth-Moulton predictor-corrector scheme [21] (consisting of a 3rd-order Adams-Bashforth predictor step and 4th-order Adams-Moulton corrector step).

The FUNWAVE model has been used for simulations of a variety of model systems, from one-dimensional small-scale wave transformation by bathymetric anomalies [28] and studies of criteria for breaking waves [29] up to the replication of the most devastating tsunamis [30]. The FUNWAVE model has been *inter alia*

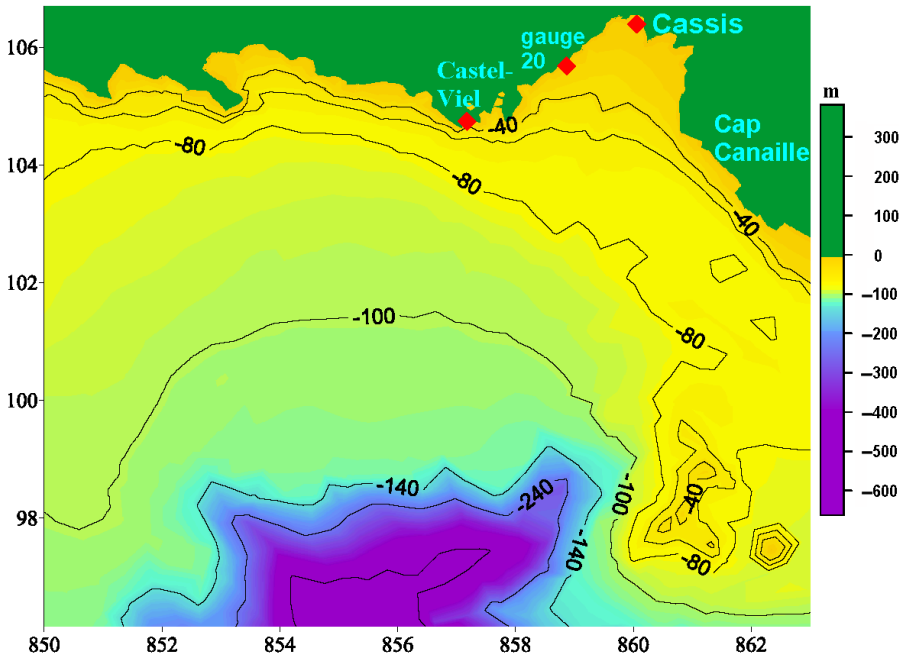

Fig. 5. Bathymetry in the vicinity of Cassis in Lambert3 coordinates (conformal conic projection; depth in m; horizontal and vertical axes in km). The grid step is 14 m in the east-west direction and 12 m in the north-south direction. The red rhombi indicate the locations of numerical gauges.

also applied to model waves, created by underwater [31,32] and subaerial [33] landslides.

The large-scale bathymetry data (Fig. 5) used in this study comes from SHOM (Service hydrographique et océanographique de la Marine). Near Cap Canaille, in shallow water (depth < 30 m), a bathymetric survey has been done by a CEREGE team with a differential real time kinematics GPS Trimble R8 and a monobeam Tritech PA500 echosounder with a resolution of a few metres across the coast and 10–20 m along the coast.

The basic assumptions and approximations used in calculations have been provided in a compact form in [20] but are repeated here for convenience. The tsunami wave, generated by a possible collapse of the cliff, was simulated using three scenarios. As we are basically interested in the order of magnitude of the tsunami danger and no detailed information is available about the potential rockfall, for the sake of simplicity it is assumed that the impact of the hypothetic cliff slump (scenario I below) is equivalent to a similar impact of an asteroid or to an impact of a sequence of smaller asteroids (scenario II). The relevant theory has been developed in [34–36]. It is assumed that the disturbance $\eta(\vec{r},0)$ to the calm water surface at $t=0$ occurs as an axisymmetric cavity of a parabolic shape expressed as [34]:

$$\begin{cases} \eta(\vec{r},0) = D_C\left(\dfrac{r^2}{R_C^2}-1\right), & r \le R_D, \\ \eta(\vec{r},0) = 0, & r > R_D. \end{cases} \tag{4}$$

Here $\vec{r}$ is the radius-vector from the axis of the cavity, $r = |\vec{r}|$, D_C is the effective cavity depth and R_C and R_D are the inner and outer radii of the cavity (the radius of the area of depression and of entire disturbed area of the water surface), respectively (Fig. 6). The disturbance, expressed by Eq. (4), is used as the initial condition for the FUNWAVE model on the background of calm water in the entire simulation area.

The maximum tsunami height occurs at the peak of the spectrum of the resulting wave system and corresponds to the following wavenumber [36]:

$$k_{\max} = \frac{2\pi}{2.11R_C}. \tag{5}$$

The relevant wavelength (about $2.11R_C$) is close to the inner diameter of the cavity. For large distances from the source it is easy to show, using the stationary phase approximation, that the maximum wave amplitude decreases with distance as r^{-1} [36]. The most powerful wave train is obtained when all the impacted water is concentrated in the bordering "lip" of the cavity. In this case, the outer and inner radii satisfy the relationship $R_D = \sqrt{3}R_C$ that is also used in our calculations[1].

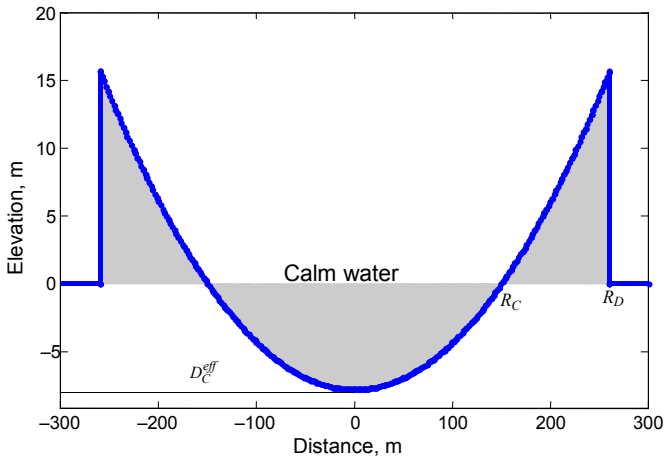

Fig. 6. Schematic cross-section of the cavity formed during a hit of a rockfall with a volume of 6×10^6 m^3 corresponding to a radius of 112 m and velocity 59.4 m/s of the impactor. The effective depth of the cavity is reduced to $D_C^{eff} = 0.85h(0)$ according to Eq. (9).

[1] This relation is presented as $R_D = \sqrt{2}R_C$ in a number of papers [34–36]. It is, however, easy to show that the volume of water in the depression of the cavity, described by Eq. (4), only equals to the volume in the bordering "lip" if $R_D = \sqrt{3}R_C$.

In reality only a certain fraction, say, ε, of the kinetic energy of the impact of the rockfall (called impactor below) is converted into the tsunami. Therefore the depth of the cavity is given by [36]

$$D_C = \sqrt{\frac{2\varepsilon\rho_i R_i^3 V_i^2}{\rho_w g R_C^2}}, \tag{6}$$

where ρ_i, R_i, and V_i are the density, radius and velocity of the impactor, respectively, g is gravity acceleration and ρ_w is the water density.

Several authors [34,35] suggest that the following relationship holds between the depth and the radius of the cavity:

$$D_C = qR_C^{\alpha}, \tag{7}$$

where q and α depend on the properties of the impactor. Substituting Eq. (7) into Eq. (6) leads to the following expression for the inner diameter $d_C = 2R_C$ of the cavity:

$$d_C = 2R_i \left(\hat{\rho}\frac{2\varepsilon V_i^2}{gR_i}\right)^{\delta} \left(\frac{1}{qR_i^{\alpha-1}}\right)^{2\delta}, \tag{8}$$

where $\delta = 1/(2+2\alpha)$ and $\hat{\rho} \equiv \rho_i/\rho_w$ is the specific density of the impactor. A reasonable estimate $\alpha = 1.27$, used in the calculations, has been obtained from laboratory experiments [34,35] and a value of $q = 0.09$ was evaluated for the typical properties of the impactor at Cap Canaille.

The parameters of the impact and the nearshore at Cap Canaille were such that the cavity depth generally exceeded the nearshore water depth. According to [34], most likely, an initial impact tsunami cannot be higher than the ocean depth, and the cavity depth cannot exceed the water depth at the impact site. For this reason the estimates of the resulting tsunami wave height are limited by the water depth [34]. Moreover, when the wave height reaches more than 86% of the water depth, the FUNWAVE model becomes unstable. This constraint gives rise to an additional restriction for the cavity depth in our calculations:

$$D_c = D_c^{eff} = \min\left[D_C(R_i),\, 0.85h(0)\right], \tag{9}$$

where $h(0)$ is the water depth at the centre of the impact site. Note that although effective cavity is limited, the inner diameter $d_C(R_i)$ of the cavity grows with the radius of the impactor.

The presented concept is only applicable for relatively high-speed impacts such as asteroids, explosions in water or (underwater) volcano eruptions [36]. It is obviously invalid for impact speeds that are comparable with the long wave speed $\sqrt{gh}$ at the impact site and under which a high "lip" of the initial disturbance cannot be formed. A rough estimate of the typical impact speed of the rupture, depicted in Fig. 3, can be obtained as a free fall speed from the

average height of the cliff (180 m). The resulting speed is about 60 m/s, which is much larger than the shallow water wave speed (10–20 m/s) in the possibly impacted area.

Physically, the limitation of the cavity depth to $D_C^{eff} = 0.85h(0)$ means that only a part of the energy of the impactors that "bottom out" the seafloor will be converted into tsunami. This limitation was used to calculate the fraction of energy $\varepsilon = 0.15$ of the impact that was converted into wave energy based on data from [35].

A collapse of the cliff may also occur in the form of a slide of a large volume of rocks along the existing cliff foot and further into the nearshore. In order to estimate the consequences of such an event, we address the possibility of tsunami generation by a subaerial sliding solid mass (scenario III). The relevant differential equation for the motion of the mass centre $x(t)$ in the direction of the source, used to describe the initial conditions for the FUNWAVE model, can be written in the form [37]:

$$WTL(\rho_i + C_m\rho_w)\frac{d^2x}{dt^2} = -WTL(\rho_i - \rho_w)gC_n - WT\frac{1}{2}\rho_w\left(\frac{dx}{dt}\right)^2 C_d\,, \qquad (10)$$

where W, T and L are the width, thickness and length of the landslide that moves in the constant-depth water with a density ρ_w. The flow velocity at the shoreline is determined from the initial velocity u, using the quadratic approximation

$$\frac{du}{dt} = -\frac{(\hat{\rho}-1)gC_n}{(\hat{\rho}+C_m)} - \frac{C_d}{2L(\hat{\rho}+C_m)}u^2\,, \qquad (11)$$

where C_m is the additional mass ratio, C_n is the Coulomb friction coefficient and C_d is the traction coefficient. We used values $C_m = 1$, $C_n = 0.5$ and $C_d = 1$, recommended in [37], and the value $L = 100$ to reflect the length of the path of the sliding solid mass. Similar formulations with slight differences in details are commonly used in other numerical studies of tsunamis excited by subaerial mass flows [32]. A more detailed analysis of the impact of such a sliding mass that enters the water along a sloping coast is performed in [38], using physical experiments and Lagrangian and Eulerian numerical models SPHysics and Gerris.

4. WAVE SIMULATIONS

As mentioned above, previous studies of past collapses suggest that the amount of hypothetical landslide is likely to range from 3 to 11 million m^3 [17]. Based on this estimate, we first evaluated the consequences of different volumes (from 3×10^6 to 11×10^6 m^3 with a step of 1×10^6 m^3) falling into the sea. The velocity $V_i \cong 60$ m/s, calculated by assuming a free fall from the average height of the cliff of 180 m, varied a little bit depending on the radius of the impactor R_i for a particular collapsing volume. In all calculations it was assumed that $\rho_i = 2\rho_w$.

The differences in the properties of waves for these values were relatively small (Table 1). Almost all the parameters (amplitude, period and arrival time to Cassis) of the resulting waves were very similar. The first wave always produced the maximum water level elevation. The arrival time of the first wave to Cassis was almost the same in all cases (cf. [38]). This suggests that the resulting wave in Cassis Bay is relatively invariant with respect to the particular collapse volume whereas even for the smallest estimated volume there will be definitely a danger for the city. As the most likely volume of the rockfall is about 6×10^6 m^3 [17], we choose this case as the triggering event of all scenarios.

As such an event not necessarily occurs instantaneously or at a single site, an alternative scenario II was designed to study the consequences of eight equal clods (each volume of 750 000 m^3) with the total volume of 6×10^6 m^3 subsequently falling into the sea along the coast within a short time interval. This scenario is quite likely according to Fig. 2: it suggests that the marl erosion occurs along a fairly long stretch at the foot of the cliff.

The third scenario III was based on the above-described model of sliding mass where the same volume of 6×10^6 m^3 was moving along the coastal slope. Thus, all scenarios correspond to the same volume of the collapsing cliff.

Top views of initial elevations derived from Eq. (4) for the first and second scenario and from Eq. (10) for the third scenario are shown in Fig. 7. The

Table 1. Parameters of the local tsunami waves near Cassis (at gauge 20, Fig. 5) for different volumes of the initial impactor for scenario I

Collapse volume, 10^6 m^3	Radius of the impactor, m	Maximum wave height, m	Arrival time of the first wave, s
3	89	1.1	190
4	98	1.5	195
5	106	1.5	195
6	112	1.5	195
7	118	1.6	195
8	124	1.4	190
9	129	1.5	195
10	133	1.8	200
11	138	1.55	195

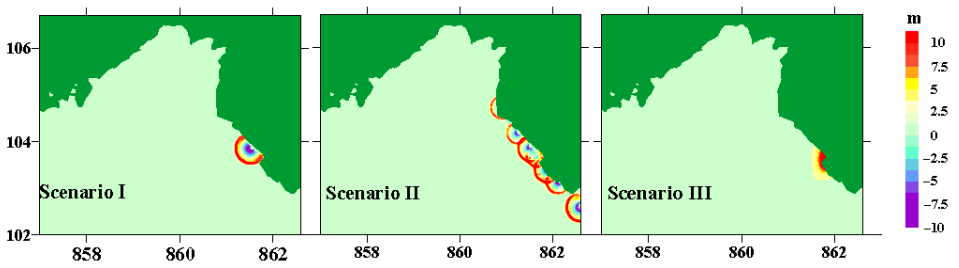

Fig. 7. The initial water surface elevation produced by a collapse of the cliff for scenarios I–III.

simulated water surface elevation was recorded at several numerical gauges at the coast (Fig. 5). These locations included points near the initial collapse site (gauges 1–4 not shown), in Cassis Bay (gauges 20–23) and also different points along Calanques (narrow fjords, gauges 11–19).

Not surprisingly, the wave patterns are similar for all the scenarios. The excited wave propagates mainly in the offshore direction but a substantial amount of wave energy propagates in the direction of Cassis. The wave front reaches the southern boundary of the computational domain (a distance of 10 km) about three to five minutes after the impact. This difference obviously stems from a slightly different location of the initial wave front in different scenarios.

The distributions of the maximum elevation and deepest depression of the water surface from its calm position are shown in Fig. 8. The elevations reach up to 8 m in the vicinity of the hypothetic slump. The largest waves propagate like cannon shots perpendicularly to the cliff, straight to the offshore. The wave amplitude decreases, as expected, relatively rapidly with distance but is still in the range of 1.5–3.6 m in Cassis Bay. Interestingly, in other bays and also at the southern, eastern and western boundaries of the model domain the wave was fairly unremarkable. Thus, the simulations suggest that the greatest waves will appear near the generation location and also in Cassis Bay.

An analysis of the time series of water level elevation at numerical gauges in Cassis (gauge 21) and Castel-Viel (gauge 19) gives further insight to what may happen in the interior of Cassis Bay after such a collapse (Fig. 9, Table 2). The first wave with a height of more than one meter and a period of 2 minutes will arrive at the city beach in about 3–3.5 minutes after the event. The maximum water level elevation may reach 3.6 m (total wave height over 4 m) if the collapse will proceed according to scenario II (collapse of several blocks). The typical period of such water level oscillations is about 30 s, that is, much smaller than

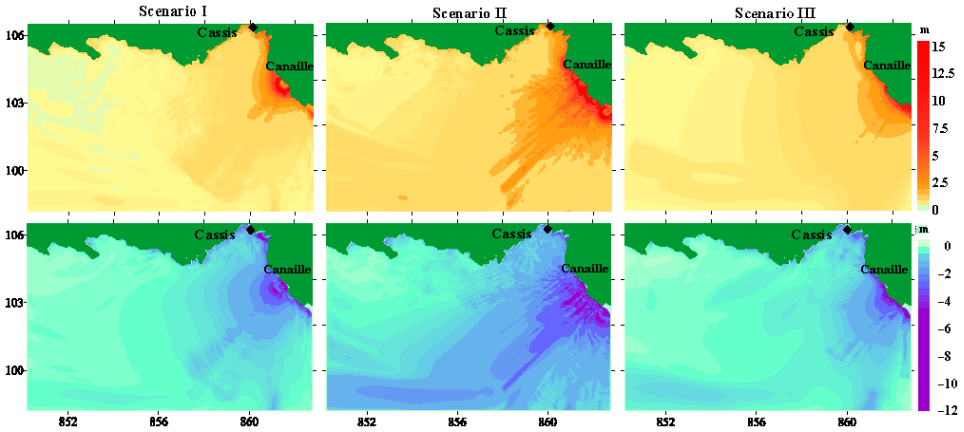

Fig. 8. Distribution of the maximum elevation (top panels) and deepest depression (bottom panels) of the sea surface over the entire time of calculations.

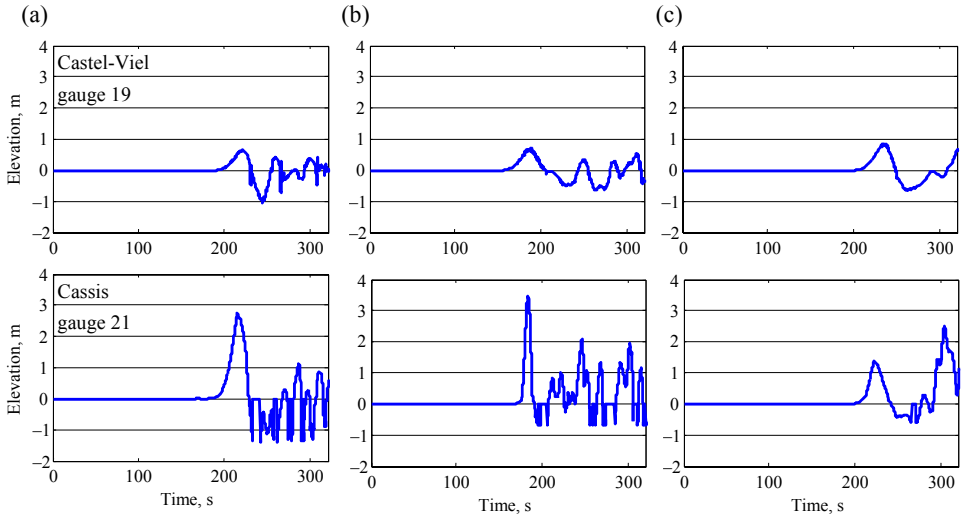

Fig. 9. Time series of water elevation at virtual gauges in Castel-Viel (gauge 19, upper panels) and Cassis (gauge 21, lower panels): (a) scenario I, (b) scenario II, (c) scenario III.

Table 2. Characteristics of tsunami waves at Cassis for scenarios I–III

Scenario	Maximum wave height, m	Arrival time of the first wave, s	Typical number of large waves
I One block	2.7	200	1
II Several blocks (total 6×10^6 m^3)	3.6	180	1
III Sliding mass	2.5	220	2

typical periods of tsunamis, which means a relatively modest range of inundation compared to long-period tsunamis. The maximum wave heights are smallest if the collapse would happen in the form of a sliding mass; in this case also the wave period is the largest. The first wave would arrive in 3 minutes if several blocks would collapse and in 4 minutes if some other scenario would occur. In all cases the first wave will produce the maximum water elevation in the city.

The presented data suggest that the overall appearance of a tsunami in Cassis Bay caused by a cliff collapse at Cap Canaille is very similar for all simulated scenarios. There are obvious differences in the arrival time and typical period of the excited waves. The major source of danger and a potential cause for loss of lives in such an event is the very short arrival time of the waves after a cliff collapse. The first, most devastating wave may arrive as rapidly as 2.5 minutes after the collapse. This short time interval hardly leaves any time for the distribution of warning message even if the collapse itself can be recognized immediately. At the same time, the height of the waves is substantial and water level elevation up to 3.6 m may occur in the case of collapse of several blocks. Such a wave is capable to cross the beach and inundate the port area, the adjacent

squares and part of streets to the city. Apart from the material damage to shops, cafes, restaurants or yachts, the small time lag means a considerable danger to the users of this area. It is most likely that there will be no warning time and the people on the beach and in the port will not know what to do and where to escape; so panic may arise, and also the possible hustle and loss of life.

5. CONCLUDING REMARKS

The presented results of simulations of several scenarios of excitation of a tsunami by a hypothetic collapse of the cliff suggest that several sections of the coastline of Cassis are in significant danger should such a collapse occur. Based on the study of past collapses [17], the recurrence time of such events may be on the order of several thousands of years, indicating a low probability for such a hazard. However, the predicted enhanced global sea-level rise may considerably shorten the time interval until the next event.

The details of the approaching waves depend on the particular features of the event to some extent but for all scenarios the overall picture of wave propagation and, consequently, the overall level of danger is basically the same. The maximum surface elevation for the Cassis region is about 3.6 m for a wide range of the collapsing volume. As many tsunamis in the past have created much larger elevations in different parts of the World Ocean, the wave attack and inundation by these relatively short-period waves would be basically manageable using classical means of tsunami hazard mitigation if there would be enough time for spreading the warning message.

The major problem for Cassis is the timing of the wave that leaves virtually no time for the warning. The arrival time of the tsunami into the harbour and beaches is as short as 2–3 minutes after the cliff collapse. Therefore, such a hypothetical event basically leaves the Cassis residents and visitors in the harbour and on the beach fully exposed to the tsunami attack.

Moreover, there is no sufficient information to accurately determine the characteristics of a potential collapse, the details of the excited wave or its particular impact zone. Some additional knowledge may be obtained by means of more appropriate modelling of the perturbation of water masses due to the landslide or rockfall. It is clear that the shape of the initial disturbance is not a sphere. Indeed, a parallelepiped or a brick, thin and long, consisting of rock, sandstone and air mixture is more appropriate. It may happen that the wave heights and surface elevations, calculated here using several rough approximations, are biased.

The major message, however, is clear: this situation calls for alternative means towards improving resilience of the potentially impacted areas along the coast of Cassis Bay. First of all, this can be achieved by extensive preparedness of the local authorities, rescue services and residents. It is definitely not enough to prepare rescue team actions towards helping people to get away from the

beach in the case of cliff collapse. The above-discussed extremely short time interval between the collapse and the arrival of the wave means that even the most well-prepared rescue services simply cannot be mobilized before the waves arrive. Therefore the focus should be on preventive activities towards preparedness of all beach and harbour users.

As the first disturbance to arrive is a wave of elevation, a warning should be given immediately based on either visual or certain sensor-based detection of the collapse. It is important that all residents would know how to proceed if such an event has been detected: to immediately abandon areas exposed to the wave attack and to move either to higher ground or to higher floors of the buildings. Moreover, they should tell the visitors of the city and beaches to do so as well. The officers should be prepared not only to help people get away from the beach towards higher ground (which effectively means walking of 100–200 m inland) but, even more importantly, to take the necessary actions to prevent panic as the wave impact and inundation time are expected to be short. The officers should be provided with the necessary equipment, transport and communications, to carry out the described activities.

We once more emphasize that focusing on a rescue alert without preparedness of the people is not reasonable due to very small time lag from cliff collapse to the arrival of waves. A passive means of mitigation of the potential damage is to further develop the protecting coastal engineering structures in Cassis in order to prevent irreparable consequences for the city infrastructure. Another important direction of efforts is the development of a monitoring system of the status of rock masses of Cap Canaille. Combined with further studies of various hypothetical events, a system of detection of motions in the cliff rocks contribute to the decisions to be taken to mitigate the local tsunami effects, such as preventive and promotional activities, to warn people about the danger, shifting the beach to a safer place, creation of rescue teams, ways to further explore and prevent the possible collapse.

ACKNOWLEDGEMENTS

We would like to thank the team of IRPHE (Marseille, France) for collaboration and fruitful discussions of the content of this work. OK acknowledges a fellowship that made possible her research stay in IRPHE. The study was also supported by the Estonian Science Foundation (grant No. 9125), targeted financing by the Estonian Ministry of Education and Research (grant SF0140007s11), and through support of the European Regional Development Fund to the Centre of Excellence in Non-linear Studies CENS, fellowship of the President of the Russian Federation to EA, and Federal Target Program “Research and scientific-pedagogical cadres of Innovative Russia” for 2009–2013 (14.B37.21.0642).

REFERENCES

1. Rahmstorf, S. A semi-empirical approach to projecting future sea-level rise. *Science*, 2007, **315**, 368–370.
2. Gornitz, V. Global coastal hazards from future sea-level rise. *Global Planet. Change*, 1991, **89**, 379–398.
3. Irish, J. L., Frey, A. E., Rosati, J. D., Olivera, F., Dunkin, L. M., Kaihatu, J. M., Ferreira, C. M. and Edge, B. L. Potential implications of global warming and barrier island degradation on future hurricane inundation, property damages, and population impacted. *Ocean Coast. Manage*, 2010, **53**, 645–657.
4. Orviku, K., Jaagus, J., Kont, A., Ratas, U. and Rivis, R. Increasing activity of coastal processes associated with climate change in Estonia. *J. Coast. Res.*, 2003, **19**, 364–375.
5. Emery, K. O. and Kuhn, G. G. Sea cliffs: their processes, profiles, and classification. *Geol. Soc. Am. Bull*., 1982, **93**, 644–654.
6. Nunes, M., Ferreira, Ó., Loureiro, C. and Baily, B. Beach and cliff retreat induced by storm groups at Forte Novo, Algarve (Portugal). *J. Coast. Res*., 2011, Special Issue 64, 795–799.
7. Orviku, K., Tõnisson, H., Kont, A., Suuroja, S. and Anderson, A. Retreat rate of cliffs and scarps with different geological properties in various locations along the Estonian coast. *J. Coast. Res*., 2013, Special Issue 65, 552–557.
8. Brooks, S. M., Spencer, T. and Boreham, S. Deriving mechanisms and thresholds for cliff retreat in soft-rock cliffs under changing climates: Rapidly retreating cliffs of the Suffolk coast. UK. *Geomorphology*, 2012, **153-154**, 48–60.
9. Fritz, H. M., Mohammed, F. and Yoo, J. Lituya Bay landslide impact generated mega-tsunami 50th anniversary. *Pure Appl. Geophys*., 2009, **166**, 153–175.
10. Hébert, H., Piatanesi, A., Heinrich, P., Schindelé, F. and Okal, E. Numerical modeling of the September 13, 1999 landslide and tsunami on Fatu Hiva Island (French Polynesia). *Geophys. Res. Lett*., 2002, **29**, Art. No. 1484.
11. Tinti, S., Manucci, A., Pagnoni, G., Armigliato, A. and Zaniboni, F. The 30 December 2002 landslide-induced tsunamis in Stromboli: sequence of the events reconstructed from the eyewitness accounts. *Nat. Hazards Earth Syst. Sci*., 2005, **5**, 763–775.
12. Pino, N. A., Ripepe, M. and Cimini, G. B. The Stromboli Volcano landslides of December 2002: A seismological description. *Geophys. Res. Lett.*, 2004, **31**, L02605.
13. Keating, B. H. and McGuire, W. J. Island edifice failures and associated tsunami hazards. *Pure Appl. Geophys*., 2000, **157**, 899–955.
14. Walder, J. S., Watts, P., Sorensen, O. E. and Janssen, K. Tsunamis generated by subaerial mass flows. *J. Geophys. Res. – Solid Earth*, 2003, **108**(B5), Art. No. 2236.
15. Ward, S. N. Landslide tsunami *J. Geophys. Res. – Solid Earth*, 2001, **106**(B6), 11201–11215.
16. Pelinovsky, E., Kharif, C., Riabov, I. and Francius, M. Modelling of tsunami propagation in the vicinity of the French coast of the Mediterranean. *Nat. Hazards*, 2002, **25**, 135–159.
17. Recorbet, F., Rochette, P., Braucher, R., Bourlès, D., Benedetti, L., Hantz, D. and Finkel, R. C. Evidence for active retreat of a coastal cliff between 3.5 and 12 ka in Cassis (South East France). *Geomorphology*, 2010, **115**, 1–10.
18. Heinrich, P., Piatanesi, A., Okal, E. and Hebert, H. Near-field modelling of the July 17, 1998 tsunami in Papua New Guinea, *Geophys. Res. Lett*., 2000, **27**, 3037–3040.
19. Khvostova O. E., Averbukh E. L. and Kurkin A. A. Cape Canaille cliff falling: hypothetic tsunami consequences estimation. In *24th International Tsunami Symposium*, Novosibirsk, 2009, 86.
20. Khvostova, O. E., Averbukh, E. L. and Kurkin, A. A. Analysis of nonseismic tsunami scenarios of the French coast of the Mediterranean Sea. *Trans. Nizhny Novgorod State Technical University n.a. R. E. Alekseev, Mechanics of Fluids and Gases*, 2010, 2(81), 49–56 (in Russian).
21. Wei, G. and Kirby, J. T. 1995. Time-dependent numerical code for extended Boussinesq equations. *J. Waterw. Port Coast. Ocean Eng*., 1995, **121**, 251–261.

22. Wei, G., Kirby, J. T., Grilli, S. T. and Subramanya, R. A fully nonlinear Boussinesq model for surface waves. Part 1. Highly nonlinear unsteady waves. *J. Fluid Mech*., 1995, **294**, 71–92.
23. Kirby, J. T. Boussinesq models and applications to nearshore wave propagation, surf-zone processes and wave-induced currents. In *Advances in Coastal Modeling* (Lakhan, V. C., ed.). Elsevier, Amsterdam, 2003, 1–41.
24. Kennedy, A. B., Chen, Q., Kirby, J. T. and Dalrymple, R. A. Boussinesq modeling of wave transformation, breaking, and runup. I: 1D. *J. Waterw. Port Coast. Ocean Eng*., 2000, **126**, 39–47.
25. Chen, Q., Kirby, J. T., Dalrymple, R. A., Kennedy, A. B. and Chawla, A. Boussinesq modeling of wave transformation, breaking and runup, II: 2D. *J. Waterw. Port Coast. Ocean Eng*., 2000, **126**, 48–56.
26. Choi, J., Lim, C. H., Lee, J. I. and Yoon, S. B. Evolution of waves and currents over a submerged laboratory shoal. *Coast. Eng*., 2009, **56**, 297–312.
27. Kirby, J. T., Wei, G., Chen, Q., Kennedy, A. B. and Dalrymple, R. A. *Funwave. Fully Nonlinear Boussinesq Wave Model. Documentation and User's Manual*. Center for Applied Coastal Research. Research Report NO CACR-98-06. 1998.
28. Bender, C. J. and Dean, R. G. Wave transformation by two-dimensional bathymetric anomalies with sloped transitions. *Coast. Eng*., 2003, **50**, 61–84.
29. D'Alessandro, F. and Tomasicchio, G. R. The BCI criterion for the initiation of breaking process in Boussinesq-type equations wave models. *Coast. Eng*., 2008, **55**, 1174–1184.
30. Ioualalen, M. Sensitivity tests on relations between tsunami signal and seismic rupture characteristics: The 26 December 2004 Indian Ocean event case study. *Environ. Modell. Softw*., 2009, **24**, 1354–1362.
31. Ioualalen, M., Pelletier, B., Watts, P. and Regnier, M. Numerical modeling of the 26 November 1999 Vanuatu tsunami. *J. Geophys. Res. Oceans*, 2006, **111**, C06030.
32. Waythomas, C., Watts, P., Shi, F. and Kirby, J. T. Pacific Basin tsunami hazards associated with mass flows in the Aleutian arc of Alaska. *Quatern. Sci. Rev*., 2009, **28**, 1006–1009.
33. Dong, G., Wang, G., Ma, X. and Ma, Y. Harbor resonance induced by subaerial landslide-generated impact waves. *Ocean Eng*., 2010, **37**, 927–934.
34. Ward S. N. and Asphaug E. Asteroid impact tsunami: a probabilistic hazard assessment. *Icarus*, 2000, **145**, 64–78.
35. Ward, S. N. and Asphaug E. Impact tsunami – Eltanin. *Deep Sea Res. II*, 2002, **49**, 1073–1079.
36. Kharif, C. and Pelinovsky, E. Asteroid impact tsunamis. *C.R. Physique,* 2005, **6**, 361–366.
37. Watts, P. and Waythomas, C. F. Theoretical analysis of tsunami generation by pyroclastic flows. *J. Geophys. Res. – Solid Earth*, 2003, **108**(B12), Art. No. 2563.
38. Viroulet, S., Cébron, D., Kimmoun, O. and Kharif, C. Shallow water waves generated by subaerial solid landslides. *Geophys. J. Int*., 2013, doi: 10.1093/gji/ggs133

Maalihke põhjustatud tsunamiga seonduvad ohud: Cassis, Prantsusmaa

Elena Averbukh, Philippe Dussouillez, Christian Kharif, Olga Khvostova, Andrey Kurkin, Pierre Rochette ja Tarmo Soomere

Ookeani veetaseme tõusu tulemusena kiireneb tõenäoliselt paljudes kohtades kõrgete rannaäärsete kaljude jalami erosioon ja need võivad ebastabiilseks muutuda. On analüüsitud Euroopa ühelt kõrgeimalt rannakaljult (394 m) Canaille' neemel Marseille' lähistel mitme miljoni kuupmeetri kaljude merre varisemise võimalikke stsenaariume. Nii varing kui ka maalihe tekitavad varingukohas mitme meetri kõrguse tsunamilaadse laine, mis väga tõenäoliselt ähvardab naab-

ruses paiknevat Cassis' linna. Laine tekkimist ja levikut on analüüsitud mitte-lineaarsetel Boussinesqi võrranditel tugineva lainemudeli FUNWAVE abil. Kõigi vaadeldud stsenaariumide puhul tabab Cassis' linna kõrge, kuni 3,6-meetrine laine. Suurimaks ohufaktoriks on asjaolu, et esimene laine, mis on ka kõrgeim, jõuab linna randadesse ja sadamasse väga kiiresti, 3–3,5 minutit pärast varingut.